Grain-Size Control in Ti-48Al-2Cr-2Nb with Yttrium Additions

P.B. TRIVEDI, E.G. BABURAJ, A. GENÇ, L. OVECOGLU, S.N. PATANKAR, and F.H. (SAM) FROES

A gas-atomized (GA) prealloyed powder of the Ti-48Al-2Cr-2Nb intermetallic and 1.6 wt pct Y were mechanically alloyed (MA) and hot isostatically pressed (hipped) to produce a fully dense nanocrystalline material. Mechanical alloying of the as-blended powder for 16 hours resulted in the formation of a disordered fcc phase. Hipping of the alloy powder produced a single-phase nanocrystalline TiAl intermetallic, containing a distribution of 20 to 35-nm-sized $Al_2Y_4O_9$ particles. The formation of oxide particles occurred by the chemical combination of Al and Y with oxygen, which entered as a contaminant during milling. Oxide particles increased the hardness of the intermetallic compound and minimized grain growth even at 0.8 T_m, where T_m is the melting point of the compound.

I. INTRODUCTION

THE lightweight intermetallic Ti-48Al-2Cr-2Nb and its modifications are potential candidates for applications in aerospace systems and automobiles, because of their low density, high elastic modulus, and high-temperature properties.[1,2,3] The major barrier to widespread use of the Ti-48Al-2Cr-2Nb alloy is the ambient lack of "forgiveness" (ductility, fracture toughness, *etc*). A secondary concern is excessive grain growth at high temperatures when present as single phase.[4] The forgiveness can be enhanced by reducing the occurrence of intragranular fracture by reducing the grain size to a nanometer scale, thereby constraining the cracks within the small grains and preventing extensive propagation. However, a small grain size can adversely affect the creep behavior, thereby potentially limiting the use of the material at high temperatures. In cast alloys, grain-size reduction can be achieved by the addition of a small amount of boron or carbon.[5] Creep resistance and a decrease in the grain growth rate in Ti alloys at temperatures even above 800 °C have been demonstrated by the addition of carbon to form appropriately distributed carbides.[5] However, it appears that the effect of a carbon addition is minimal at temperatures above 850 °C, due to the instability of the carbide particles.[5] More effective control of the grain growth should be possible by using a dispersion of fine yttria particles, which are generally more stable than carbides in a titanium matrix;[6,7] yttria particles have been used successfully to control grain size in conventional alloys such as Ti-6Al-4V. A dispersion of thermally stable particles would also increase the strength of the alloy at high temperatures.[6,7]

Dispersion strengthening is achieved by producing a dispersion of thermally stable particles in the matrix by mechanical alloying, solidification processing, or other techniques including electro- or electroless deposition. In the mechanical alloying process, the repeated welding, fracturing, and rewelding of powder particles mixes the powders on an atomic scale, leading to true alloying.[8–13] Oxide-dispersion-strengthened alloys, which are MA with yttria, possess excellent properties compared to conventional ingot-metallurgy material.[14,15] When present as a uniform dispersion, yttria additions retard recrystallization after hot working by blocking dislocation motion.[16]

Major concerns in the dispersion of oxide particles by mechanical alloying are (1) oxygen contamination in the as-milled powder, (2) limitations in the size reduction of oxide particles, and (3) the uniformity of the distribution of oxide particles. Oxygen contamination in the matrix alloy can be minimized if the contaminant oxygen can be used to form a uniform distribution of stable oxides. A process to distribute yttrium oxides by the dissolution of metallic yttrium in oxygen containing Ti alloys, followed by solidification to precipitate oxides, was demonstrated earlier.[17,18] In the case of an *X*-127 alloy (Ni-16Cr-4.5Al-1Y), Raghaven *et al.*[18] demonstrated the formation of a mixed Al-Y-O oxide in the alloy matrix, in preference to a yttrium or aluminum oxide. The present work is an attempt to mechanically alloy yttrium with the TiAl intermetallic and then consolidate the alloy, to form a fine dispersion of yttrium–aluminum oxide particles, by consuming the oxygen that enters as a contaminant during processing. The availability of all Al, Y, and O in the mechanically alloyed system is expected to result in the formation of a uniform distribution of the mixed oxide.

II. EXPERIMENTAL

All the experimental work reported in this paper was carried out at the Institute for Materials and Advanced Processes (IMAP), University of Idaho, Moscow, Idaho. An as-blended gas-atomized (GA) Ti-48Al-2Cr-2Nb powder and 1.6 wt pct Y were MA for different times at room temperature in a SPEX 8000 high-energy ball mill. About 1 pct stearic acid ($C_{18}H_{36}O_2$) was added as process control agent, so as to prevent excessive cold welding between the powder particles, grinding media, and container walls. The vial was loaded with the as-blended powder and sealed with insulation tape inside an argon atmosphere to reduce atmospheric contamination. The ratio of grinding media (hardened 52100 steel balls) to the powder mixture was kept as 10:1 in all the experiments. The vial was rotated by 90 deg every 30 minutes and was continuously cooled externally by a table fan to minimize heating of the powder inside the vial. The

P.B. TRIVEDI, Graduate Student, S.N. PATANKAR, Research Assistant Professor, and F.H. (SAM) FROES, Director, are with the Institute for Materials and Advanced Processes, University of Idaho, Moscow, ID 83844. E.G. BABURAJ, Research Associate Professor, is with the Department of Mechanical Engineering, University of Houston, TX 77204. Contact e-mail: braj@uh.edu A. GENÇ, Graduate Student, and L. OVECOGLU, Professor, are with the Istanbul Technical University, Maslak-Istanbul, Turkey 80626.

Manuscript submitted October 9, 2001.

MA powders were then removed in an argon atmosphere inside a glove bag. Hipping of powder MA for 16 hours was carried out at 785 °C for 1 hour and at 1030 °C for 2 hours at a 207 MPa pressure.

The hipped sample was prepared for optical microscopy using the standard metallographic technique and was then etched for 8 seconds using a solution containing 96 mL distilled water, 2 mL HF, and 2 mL HNO_3. An Hitachi S-2300 scanning electron microscope (SEM) was used to examine the morphology and particle size of the as-blended and milled powders.

Grain growth of the hipped samples was examined after isothermal heat treatments under an argon atmosphere at 1050 °C for different times. Two slices of the hipped sample were wrapped with zirconium foil and vacuum sealed in silica glass tubes. These samples were heated in a horizontal electric furnace at 1150 °C for 30 minutes and 3 hours, respectively, and were quenched in chilled water. Microstructural characterization of the powder material, hipped samples, and heat-treated compacts was conducted using a JEOL* JEM 2010 transmission electron microscope (TEM) attached to a LINK ISIS microanalysis system. Thin foils for the TEM were prepared by electropolishing using an electrolyte solution consisting of 30 mL perchloric acid (30 pct), 175 mL n-Butyl alcohol, and 300 mL methanol, cooled to −40 °C at 50 V settings in a Fischione twin-jet electropolishing unit. Phase analysis and lattice-parameter calculations of the samples were carried out by X-ray diffraction (XRD) using a Siemens D5000 high-resolution diffractometer. Microhardness measurements of the hipped samples and heat-treated samples were carried out using a 500-g load for 20 seconds.

*JEOL is a trademark of Japan Electron Optics Ltd., Tokyo.

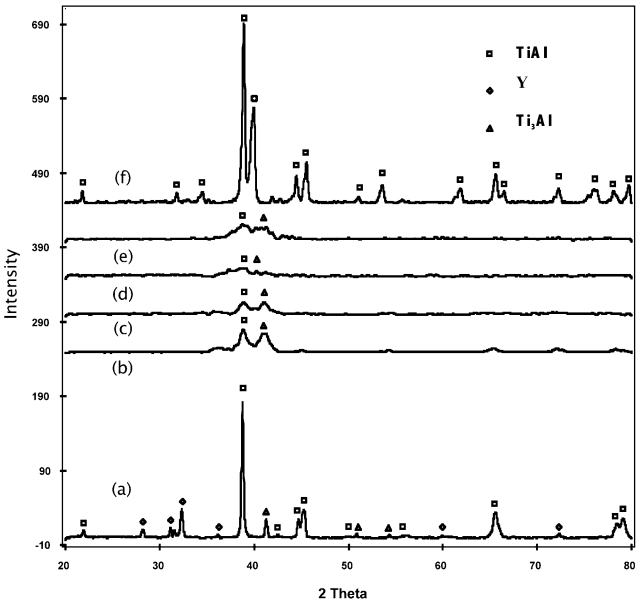

Fig. 1—XRD pattern showing broadening of TiAl peaks with an increase in milling times: (*a*) as-blended GA Ti-48Al-2Cr-2Nb + 1.6 wt pct Y powder, (*b*) powder milled for 2 h, (*c*) powder milled for 4 h, (*d*) powder milled for 8 h, (*e*) powder milled for 16 h, (*f*) hipped compact of the powder milled for 16 h.

Table I. Calculation of Lattice Parameter of TiAl from XRD Patterns for Powders Milled for 4 and 8 Hours

Milling Time	*a* (nm)
4 h MA powder	0.4017
8 h MA powder	0.4016

III. RESULTS

A. *As-Milled Powder*

Figure 1 shows the XRD patterns of the Ti-48Al-2Cr-2Nb and 1.6 wt pct Y powder as a function of milling time. The as-blended powder essentially consisted of γ-TiAl, along with a small amount of Ti_3Al phase and Y in elemental form. Significant broadening of the TiAl and Ti_3Al peaks was observed with increasing milling time. The XRD pattern after 4 hours of milling showed two strong peaks at 2θ values of 39 and 41 deg. These two peaks further broadened with an increase in milling time, as shown in Figures 1(d) and (e). The lattice-parameter calculations from the XRD pattern of the powders milled for 4 hours and 8 hours is shown in Table I. The lattice parameter was not determined for the powder milled for 16 hours, because of the large width of the peaks and the consequent uncertainties associated with determining the peak position. Chemical analysis of the powder milled for 16 hours showed 0.37 wt pct oxygen, as compared to 0.09 wt pct in the starting powder.

Figure 2 shows SEM photomicrographs of the as-blended, GA Ti-48Al-2Cr-2Nb powder and the 1.6 wt pct Y, and of the powder after milling for 1, 2, 4, and 16 hours, indicating that the average particle size continuously decreased with milling time. The shape of the as-blended powder particles is nearly spherical, while it is irregular for the milled powder. Structural details of the fine powder after 16 hours of milling are shown in the TEM bright- and dark-field photomicrographs of an electron-transparent particle in Figure 3.

The diffraction pattern from the particle (Figure 3(c)) shows a set of continuous rings, indicating a random orientation of the ultrafine grains forming the particle. An analysis of the ring pattern suggests that the milled powder has an fcc structure. The calculated *d* values for the different sets of hkl planes and the lattice parameter (*a*) are given in Table II. Even though a TEM powder-diffraction pattern does not give a reliable lattice parameter, the consistency in the values in the last column in Table II confirms the fcc structure of the milled powder. The dark-field photomicrograph obtained by imaging a portion of the first and second intense rings in Figure 3(c) is shown in Figure 3(b). The individual grains in the particle are seen as fine, bright crystals with a size in the range of 5 to 7 nm. The chemical analysis of the powder for metallic elements using energy-dispersive spectroscopy (EDS) in the TEM showed the composition (in at. pct) to be Ti-41.2Al-11.4Nb-3.8Cr-0.5Y.

B. *Consolidated and Heat-Treated Samples*

Figure 1(f) shows the XRD pattern of the as-hipped compact after 16 hours of milling. Most of the peaks in the pattern match with γ-TiAl; however, one extra peak, marked

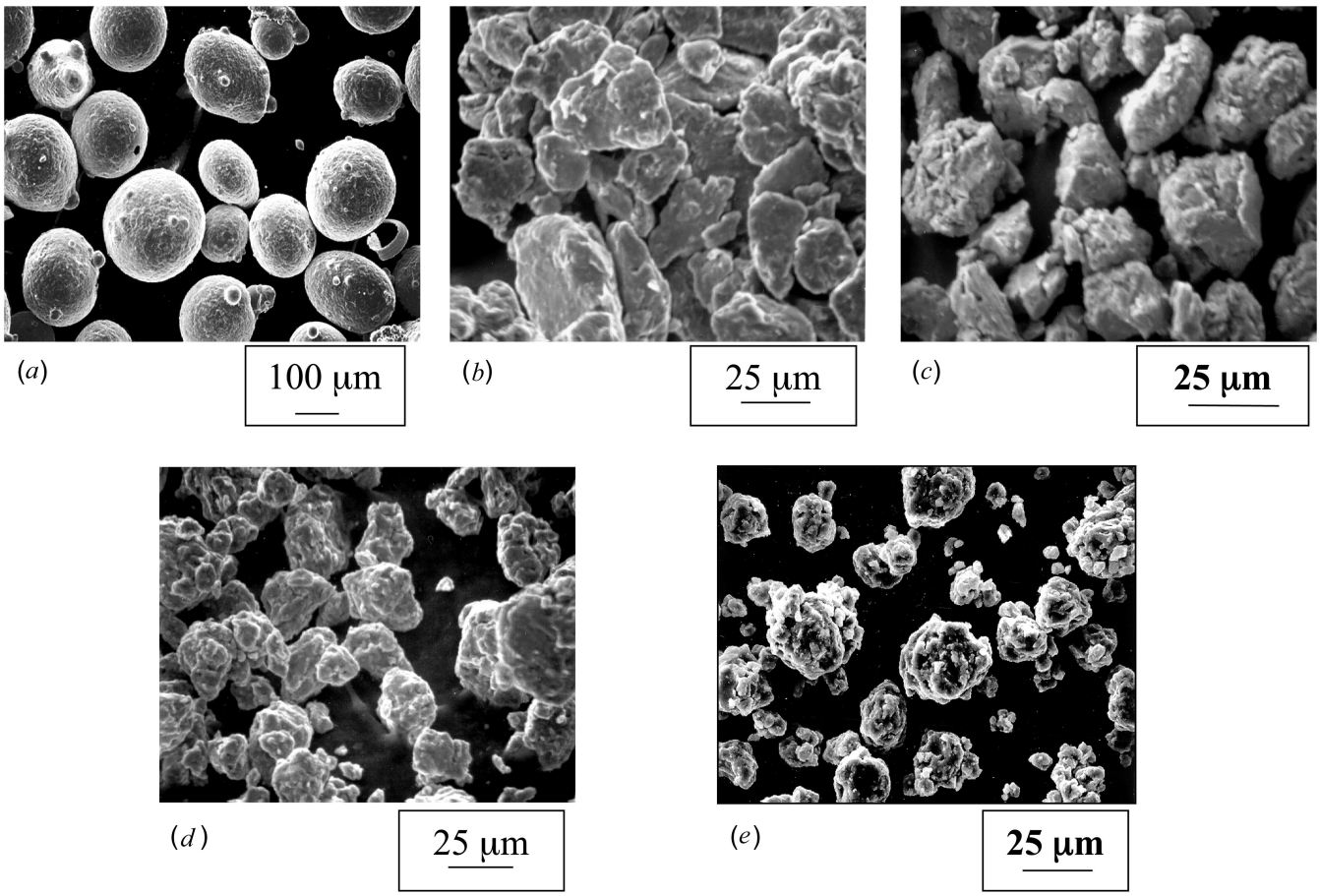

Fig. 2—(*a*) SEM photomicrograph of coarse as-blended Ti-48Al-2Cr-2Nb + 1.6 wt pct Y powder particles, (*b*) powder milled for 1 h, and (*c*) powder milled for 2 h, (*d*) powder milled for 4 h, and (*e*) powder milled for 16 h.

"o," could not be identified. The presence of Y in either the metallic or oxidized form was not detected. The lattice parameters of the TiAl phase after hipping are $a = 0.3967$ nm and $c = 0.4120$ nm, as compared to the starting powder, with $a = 0.3976$ nm and $c = 0.4049$ nm.

Examination of the hipped compact using the TEM (Figure 4(a)) showed very fine equiaxed grains of γ-TiAl, with an average grain size of about 100 nm. A distribution of fine, second-phase particles in the size range of 20 to 35 nm is evident in the figure. The EDS analysis of the fine particles using the TEM qualitatively confirmed the presence of the high Y, O, and Al content of the particles as compared to the matrix.

Figures 4(b) and 4(c) show TEM photomicrographs of the hipped compact after heat treatment at 1050 °C for 8 and 16 hours, respectively, illustrating grain growth and an uneven size distribution of the oxide particles. It is assumed that coarser particles nucleated first and grew during heat treatment, along with the nucleation of new fine particles. An estimate of the average grain size of samples after hipping and heat treatment is given in Table II and plotted in Figure 6(a). The average grain sizes after heat treatments at 1050 °C for 8 hours and 16 hours are 284 and 297 nm, respectively. The hardness values of these samples are plotted in Figure 6(b) as a function of heat-treatment time. The as-hipped compact has the highest hardness of 923 Hv, which decreased to 878 and 839 Hv after isothermal annealing at 1050 °C for 8 and 16 hours, respectively.

C. *Oxide Particles*

The fraction of the oxide particles after heat treatment for the longest period of 16 hours at 1050 °C was 16 pct. The exact chemical analysis of the particles is difficult to determine because the particles are normally embedded within the matrix, and any chemical analysis shows the combined chemistry of both the particles and the matrix. The hipped sample was heat treated at a high temperature of 1150 °C for 3 hours and water quenched at a very fast rate in order to test the dissolution of fine particles into the matrix. The TEM photomicrograph of the quenched sample contained large thin areas, including fine particles projecting into the hole formed during thinning. An individual particle projecting from a grain in shown in Figure 5(b), and EDS analysis of the particle using a 5 nm electron beam showed the ratio of the atomic percentages of the constituent elements (Al:Y:O) to be close to 2:4:9. Figure 5(c) shows the diffraction pattern taken from the same particle. The diffraction pattern corresponds to the ⟨001⟩ zone axis of $Al_2Y_4O_9$, with an orthorhombic structure and lattice parameters of $a = 1.046$ nm, $b = 1.0546$ nm, and $c = 0.3680$ nm. A computer-simulated diffraction pattern of the orthorhombic structure corresponding to the ⟨001⟩ zone axis is also shown in Figure 4(d) for comparison. The oxide particles formed randomly within the grains, at the grain boundaries, and at the triple junctions.

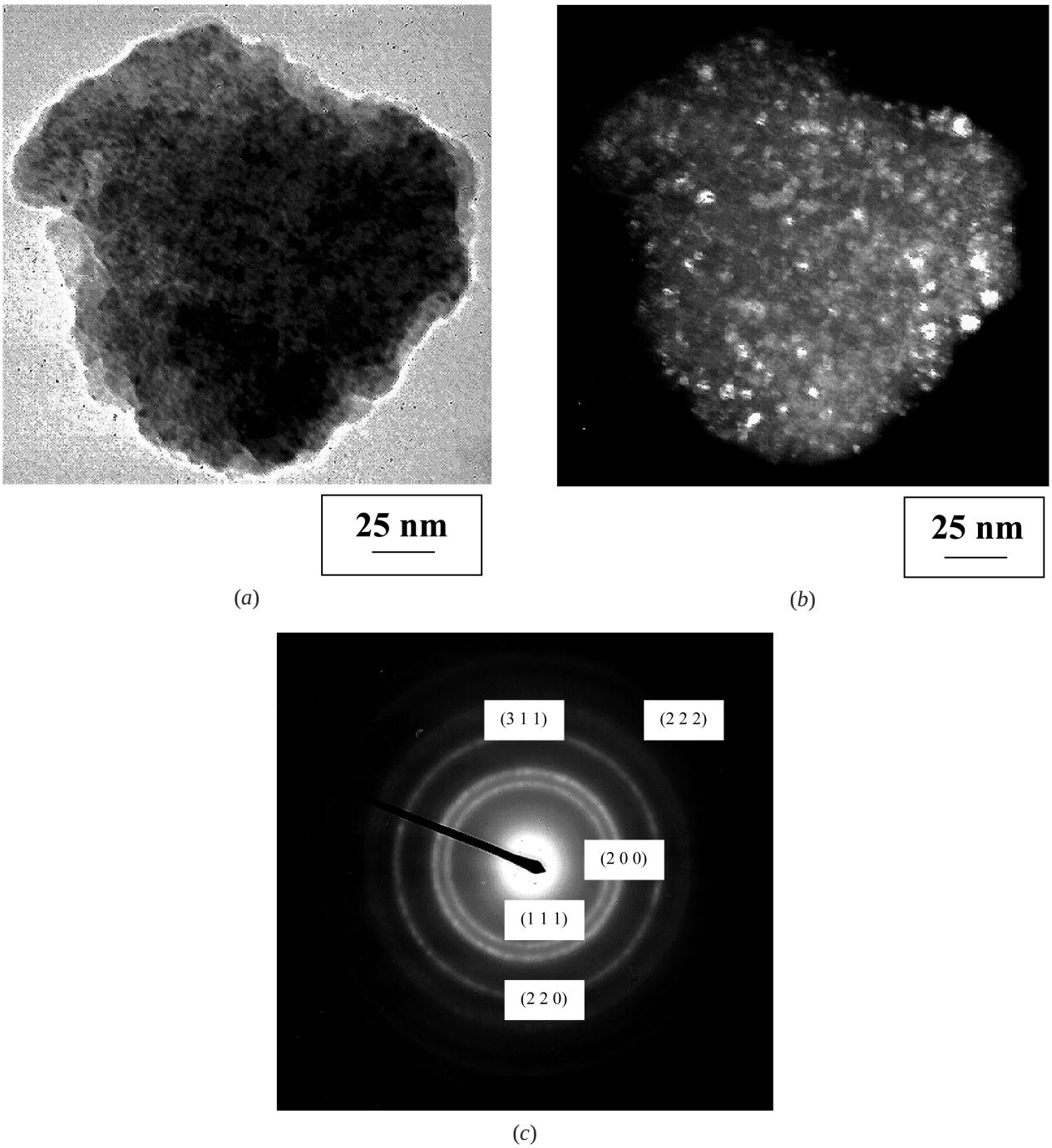

Fig. 3—TEM photomicrographs of Ti-48Al-2Cr-2Nb + 1.6 wt pct Y powder milled for 16 h: (*a*) BF, (*b*) DF showing nanoscale grains, and (*c*) corresponding diffraction pattern.

Table II. Calculation of *d* Spacing and Corresponding Lattice Parameter from Ring Diffraction Pattern of Powder Milled for 16 h

Ring	Plane	*d* Spacing (nm)	Lattice Parameter *a* (A)
1	(1 1 1)	0.227	0.393
2	(2 0 0)	0.196	0.392
3	(2 2 0)	0.138	0.392
4	(3 1 1)	0.119	0.394
5	(2 2 2)	0.113	0.393

IV. DISCUSSION

A. *Mechanical Alloying*

The disappearance of Y in the MA powder is consistent with earlier observations in many similar systems, in which small amounts of a ductile metal disappear after milling.[6] In the present case, milling of hard titanium aluminide with soft Y resulted in alloying of the metal with the intermetallic. A detailed chemical analysis of individual crystals in the MA sample seen in Figure 3(c) is not possible because of the presence of a large number of such fine subgrains within the thickness of the agglomerate. It is assumed that Y has

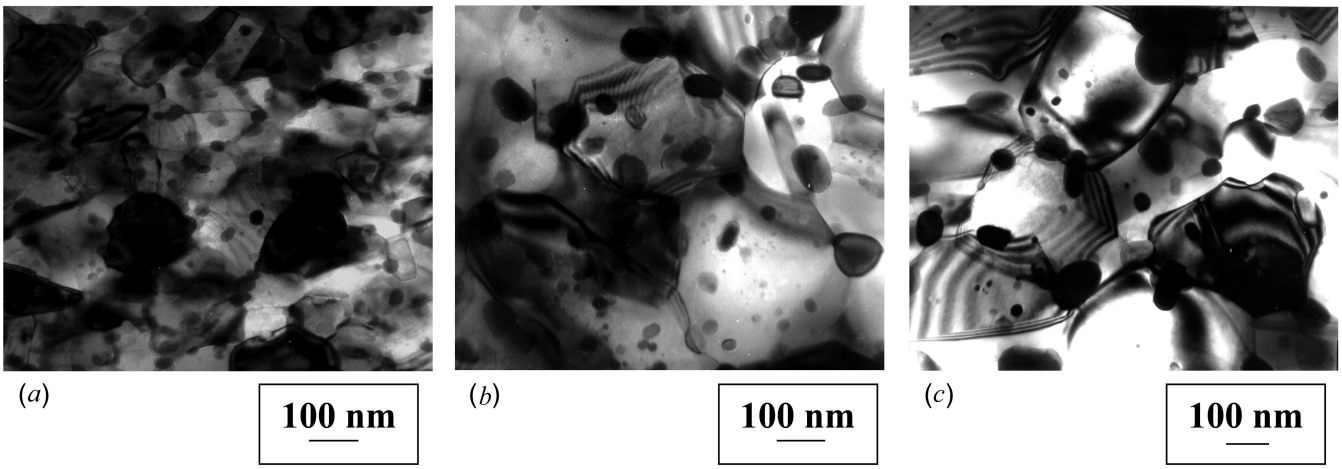

Fig. 4—TEM photomicrographs of Ti-48Al-2Cr-2Nb with 1.6 wt pct Y milled for 16 h: (*a*) hipped at 1030 °C, (*b*) heat treated at 1050 °C for 8 h, and (*c*) heat treated at 1050 °C for 16 h. A small increase in grain size is seen after the heat treatment.

Table III. Effect of Heat Treatments on Grain Size of TiAl, Calculated from TEM Photomicrographs

Sample	Grain Size (nm)
As hipped	102
8 h annealing at 1050 °C	284
16 h annealing at 1050 °C	297

gone in solution with the aluminide. The transformation of the ordered fct structure of Ti-48Al-2Cr-2Nb to the disordered fcc structure is shown in the electron diffraction pattern (Figure 3(c)). A similar order-to-disorder transformation by milling has been observed in various other systems.[19–23] The XRD patterns indicate that the disordering transformation is incomplete for milling times of 1 and 2 hours, and the lattice-parameter measurements were not carried out for these samples. The lattice parameters derived from powders milled for 4 and 8 hours have been chosen for the confirmation of the disordered structure after milling. Extensive broadening of the XRD peaks, due to severe plastic deformation and the fine size of subgrains in the powder milled for longer time, makes structural identification of the milled powder difficult. However, the consistency in the *a* value (Table I) corresponding to samples milled for shorter times confirms disordering of the intermetallic compound, more convincingly than that indicated by the selected-area diffraction patterns (Figure 3(c)).

B. *Consolidation by Hipping*

Consolidation of the milled powder by hipping at 1030 °C for 2 hours resulted in the following transformations: (1) the disordered fcc to ordered fct structure, (2) the formation of mixed oxide ($Al_2Y_4O_9$) particles in the matrix, and (3) the growth of matrix and oxide particles. The ordering transformation is an exothermic process and can occur at temperatures well below the hipping temperature.[24] Therefore, the disorder-to-order transformation might have occurred prior to the growth of matrix grains as well as the oxide particles. It is not clear whether the oxide particles nucleated prior to, during, or after the ordering transformation during hipping.

C. *Grain Growth*

The increase in average grain size of the milled powder (3 to 5 nm) during consolidation (102 nm) confirms the grain growth under the conditions of high temperature and pressure during hipping. The grain growth from 5 to 102 nm could be an effect of extensive disorder and the consequently high diffusion rates within the fine particles. Senkov *et al.*[25] studied the effect of temperature on grain size of an alloy of similar composition without any oxide dispersion. In their study, the average grain size of the milled compact after a heat treatment at 1100 °C for 5 hours increased to 541 nm, while the grain growth rate in the present study was considerably lower. A higher heat-treatment temperature of 1150 °C for 3 hours, in the present case, resulted in a maximum grain size of about 300 nm. The slow grain growth can be attributed to the pinning effect of the $Al_2Y_4O_9$ particles. A similar pinning effect has been observed in various Al systems[26,27] and Ti-6Al-4V,[28] due to second-phase particles. Zener and Smith[19] developed a quantitative theoretical expression for the critical grain size as a function of the average size and volume fraction of second-phase particles. The grain boundary stops moving when the driving force for growth equals the retarding force due to the second-phase particles.[19] In the present case, an effective pinning force due to dispersed $Al_2Y_4O_9$ particles is imposed on the TiAl system, and the grain growth rate is reduced.

D. *Oxide Phase Formation*

The pinning effect of $Al_2Y_4O_9$, determined in the present study, is considerably larger as compared to that of TiC formed in TiAl-based alloys by the addition of a small amount of carbon.[5] In the case of alloys containing TiC, the creep resistance at temperatures above 850 °C is reduced drastically due to the coarsening and dissolution of the carbides.[5] The present observation of the high stability of $Al_2Y_4O_9$ is consistent with similar observations made on the $Al_5Y_3O_{12}$-dispersed Ti-based alloys.[18] Compared to Y_2O_3, the Al-containing oxide has higher thermal stability[18] and, therefore, can result in higher creep resistance and reduced grain growth. Chemical homogeneity in terms of the oxygen content in the as-milled powder at the 5 nm scale indicates

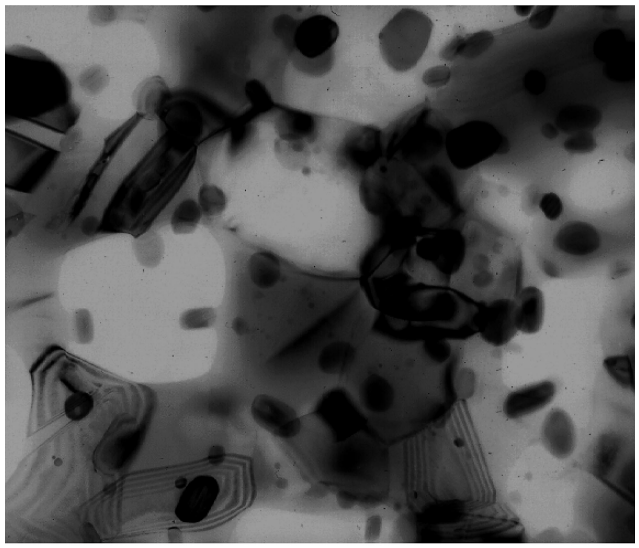

(*a*)

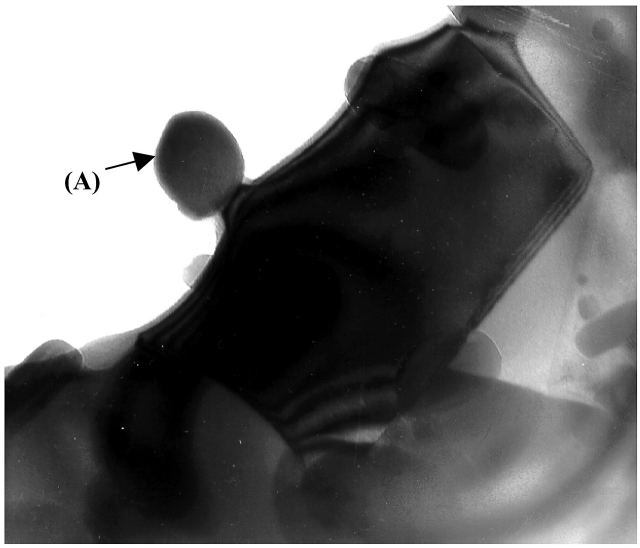

(*b*)

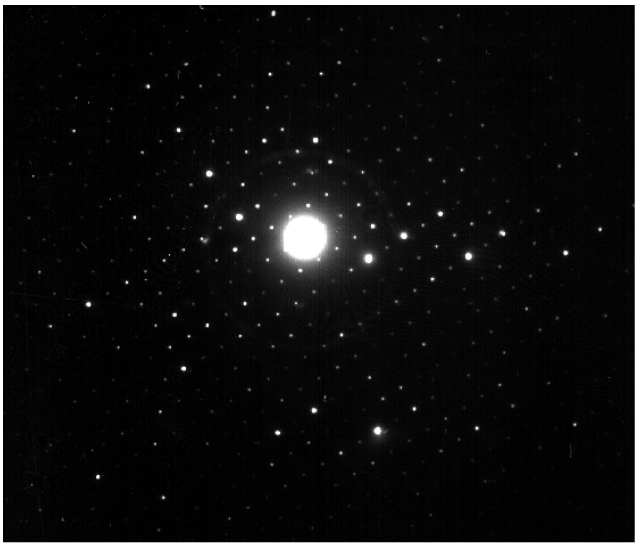

(*c*)

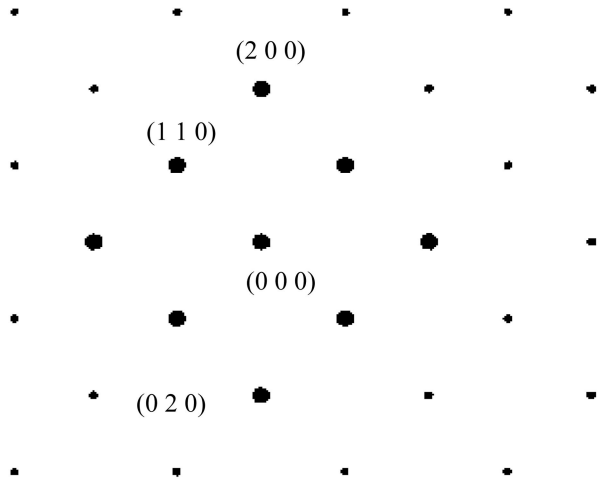

(*d*)

Fig. 5—TEM photomicrographs of hipped compact heat treated at 1150 °C for 3 h and water quenched showing (*a*) absence of dissolution of oxide particles, (*b*) an oxide particle (A) projecting from the matrix, (*c*) diffraction pattern taken from region (A), and (*d*) computer simulated key for orthorhombic structure with zone axis ⟨001⟩.

the absence of oxide particles prior to compaction. Therefore, the elements forming the oxide particles should have been uniformly distributed within the fine powder particles. The sources of oxygen in the sample are the oxide layers on the starting titanium aluminide and Y powders and contamination occurring during milling. A number of oxide particles (Figure 4) attached to the grain boundaries are large in size compared to those within the grains. This observation suggests preferential diffusion of Y along grain boundaries. Possible fast diffusion of Y along grain boundaries has been suggested elsewhere[17] in a Ti alloy, and a similar mechanism could be operative in the present case.

The preferential movement of oxygen atoms toward the oxide particles during growth can be expected to continuously deplete the oxygen present in the intermetallic matrix. Thus, it could be suggested from the present experiment that the oxide formation through the addition of elemental Y contributes to minimize oxygen contamination in the metal matrix.

E. *Volume Fraction of Oxide Particles*

The volume fraction of $Al_2Y_4O_9$ particles corresponding to 1.6 wt pct Y in the alloy, based on chemistry, is 8 pct. The reason behind the disagreement between the ideal value and that calculated from experiments is the fact that the

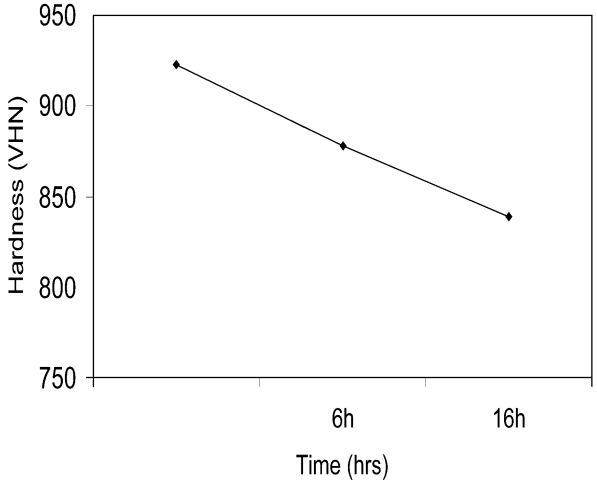

(*a*)

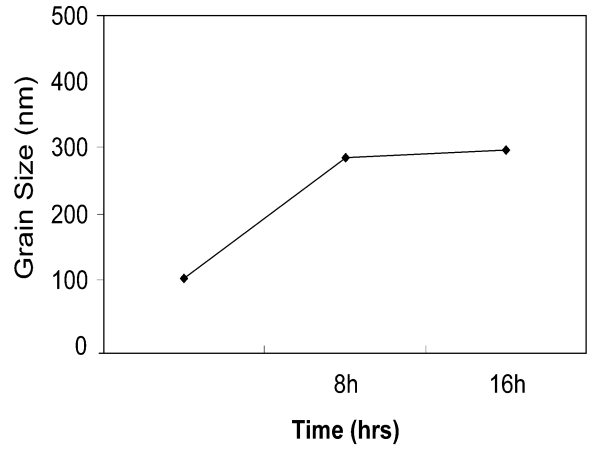

(*b*)

Fig. 6—Effect of isothermal heat treatment time at 1050 °C on (*a*) hardness of the hipped compact and (*b*) grain size of the hipped compact.

evaluation did not take into consideration the foil thickness. The fraction was evaluated on the basis of the fractional area occupied by the particles. This method of evaluation takes into consideration not only the particles on the surface, but also the particles in the interior of the thin foil. Compared to the calculated value of 8 pct, the observed value (16 pct) is significantly larger, revealing the possibility that all of the yttrium in the starting powder has been consumed. The absence of yttrium in the TiAl matrix, determined by EDS analysis after 16 hours of heat treatment at 1050 °C, further confirms the complete consumption of Y for the formation of $Al_2Y_4O_9$. The yttrium addition simultaneously contributes to the removal of oxygen from the matrix and enhancement of strength properties through precipitation of oxide particles.

V. CONCLUSIONS

The overall process of the nanocomposite formation can be summarized as

$$\text{Ti-48Al-2Cr-2Nb/Y} \xrightarrow[\textit{Mechanical Alloying}]{} \text{disordered fcc} \xrightarrow[\textit{Hipping}]{} \text{ordered TiAl} + Al_2Y_4O_9$$

The following specific conclusions have been derived from the experimental results.

1. Mechanical alloying of Ti-48Al-2Cr-2Nb with 1.6 wt pct Y reduces the grain size to about 7 nm.
2. Mechanical alloying resulted in the transformation of the ordered fct structure of the intermetallic to a disordered fcc structure.
3. Hipping leads to the formation and the uniform dispersion of fine $Al_2Y_4O_9$ particles into the nanocrystalline TiAl-based intermetallic metal matrix.
4. The oxide particles form by the chemical combination of Y and Al with the oxygen, which enters as a contaminant.
5. The pinning effect of hard $Al_2Y_4O_9$ particles retards grain growth even at a temperature of 0.80 T_m (1150 °C), where T_m is the melting point of the alloy.
6. The oxide particles grow at all the heat-treatment temperatures examined in this study.
7. The growth of oxide particles appears to consume oxygen from the matrix alloy.
8. The hardness of the nanocomposite decreases with an increase in the size of grains and the fine oxide particles.
9. The present study indicates the possibility of producing nanocrystalline composites of titanium aluminides with a mixed oxide by incorporating Y into the alloy powder as an alloying element.

REFERENCES

1. F.H. Froes, C. Suryanarayana, and D. Eliezer: *J. Mater. Sci.*, 1992, vol. 27, pp. 5113-40.
2. S. Naka, M. Thomas, and T. Khan: *Mater. Sci. Technol.*, 1992, vol. 8, pp. 291-98.
3. D.M. Dimiduk, D.B. Miracle, and C.H. Ward: *Mater. Sci. Technol.*, 1992, vol. 8, pp. 367-75.
4. H. Mabuchi, H. Tsuda, Y. Nakayama, and E. Sukedai: *J. Mater. Res.*, 1992, vol. 7, pp. 894-900.
5. Y.-W. Kim and D.M. Dimiduk: *Int. Symposium on Advanced Materials (ISAM)- International Conference on Engineering & Technological Sciences*, (2000), Beijing, Oct. 11-13, 2000.
6. P.L. Threadgil and B. Wilshire: *Met. Sci. J.*, 1974, vol. 8, pp. 117-24.
7. J.D. Parker and B. Wilshire: *Met. Sci. J.* 1975, vol. 9, pp. 248-52.
8. C.C. Koch: *Ann. Rev. Mater. Sci.*, 1989, vol. 19, pp. 121-43.
9. C.C. Koch: *Mater. Sci. Technol.*, 1991, vol. 15, pp. 193-245.
10. C. Suryanarayana and F.H. Froes: *Mater. Sci. Forum*, 1992, vols. 88–90, pp. 445-52.
11. P.H. Shingu, B. Huang, S.R. Nishitani, and S. Nasu: *Trans. Jpn. Inst. Met.*, 1988, vol. 29, pp. 3-10.
12. F.H. Froes, C. Suryanarayana, G.H. Chen, A. Frefer, and G. Hyde: *J. Mater. Sci.*, 1992, vol. 44, pp. 26-29.
13. C. Suryanarayana, C.R. Sundaresan, and F.H. Froes: *Adv. Powder Metall.*, 1989, pp. 175-88.
14. E. Arzt: *Res. Mech.*, 1991, vol. 31, pp. 399-453.
15. J. Rosler and E. Arzt: *Acta Metall.*, 1980, vol. 71, pp. 671-83.
16. G.E. Dieter: *Mechanical Metallurgy*, 3rd ed., McGraw-Hill Book Company Ltd., London, 1988, pp. 212-19.
17. S. Naka, H. Octor, E. Bouchand, and T. Khan: *Scripta Metall.*, 1989, vol. 23, pp. 501-05.
18. M. Raghaven, J.W. Steeds, and R. Petkovicluton: *Metall. Mater. Trans. A*, 1982, vol. 13A, pp. 953-57.
19. H. Bakker and L.M. Di: Mater. *Sci. Forum*, 1992, vols. 88–90, p. 27; Zener private communication to C.S. Smith: *Trans. Am. Inst. Min. Eng.* vol. 175, 1948, p. 47.
20. J.S.C. Jang and C.H. Tsau: *J. Mater. Sci.*, 1993, vol. 28, pp. 982-88.
21. W. Guo, A. Iasonna, M. Magini, S. Martelli, and F. Padella: *J. Mater. Sci.*, 1994, vol. 29, pp. 2436-44.
22. W. Guo, S. Martelli, F. Padella, M. Magini, N. Burgio, E. Paradiso, and U. Franzoni: *Mater. Sci. Forum*, 1992, vols. 88–90, pp. 139-46.

23. C.C. Koch: *Mater. Sci. Forum*, 1992, vols. 88–90, pp. 243-62.
24. H. Ogawa, K. Omuro, and H. Miura: *Mater. Sci. Forum*, 1995, vols. 179–181, pp. 781-86.
25. O.N. Senkov, N. Srisukhumbowornchai, L. Ovecoglu, and F.H. Froes: *Scripta Mater.*, 1998, vol. 39, pp. 691-98.
26. M. Goncalves: *Scripta Metall. Mater.*, 1991, vol. 25, pp. 835-40.
27. A. Waheed and G.W. Lorimer: *J. Mater. Lett.*, 1997, vol. 16, pp. 1643-46.
28. F.H. Froes, C.M. Cooke, D. Eylon, and K.C. Russell: *Titanium Sci. Technol.*, 1988, vol. 31.